Linked Nickel Metallacrowns from a Phosphonate/2-Pyridyloximate Blend of Ligands: Structure and Magnetic Properties

Albert Escuer,[*,†] Júlia Mayans,[†] and Mercè Font-Bardia[‡]

†Departament de Química Inorgànica and Institut of Nanoscience and Nanotechnology (IN2UB), Universitat de Barcelona, Avenida Diagonal 645, Barcelona 08028, Spain

‡Departament de Mineralogia, Cristallografia i Dipòsits Minerals and Unitat de Difracciódе R-X, Centre Científic i Tecnològic de la Universitat de Barcelona, Martí Franqués s/n, 08028 Barcelona, Spain

ABSTRACT:

In the present work, four new NiII clusters with nuclearities ranging between Ni4 and Na2Ni8 were synthesized, employing the versatile ligand phenylphosphonate and 6-methylpyridylaldoximate as the coligand. Crystallographic data show that the tetranuclear complex [N i 4 (6 - MepaoH)4(PhPO3)2(OH)2(MeOH)4](OH)2 (1) consists of two dimers linked by phosphonate bridges, whereas [Cs2Ni6(6-epao)6(PhPO3)3(OH)2(H2O)8] (2), Cs[Ni8(6-MepaoH)6(6-Mepao)6(PhPO3)3](ClO4)5 (3), and [Ni8Na2(BzO)6(6-Mepao) 6(PhPO3)3] (4) are built from phosphonato-linked {Ni3(6-Mepao)3} metallacycles. The [9-MCNiII(6-Mepao)-3] fragments in 2−4 show the unusual coordination of additional Cs+, Na+, and/or NiII cations. Direct-current magnetic measurements were carried in the 300−2 K range. Analysis of the experimental data revealed a complex response with strong antiferromagnetic interactions mediated by the oximato bridges and weak interactions mediated by the phosphonate ones.

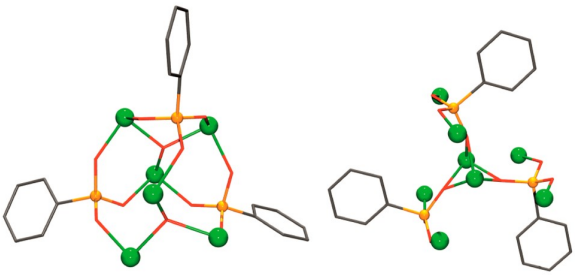

INTRODUCTION

The syntheses and characterization of 3d or 4f metallic clusters are a continuously growing subject because of their intrinsic interest and relevance in a variety of research fields such as bioinorganic chemistry1 or molecular nanomagnetism.2 The need of more examples of systems exhibiting single-moleculemagnet (SMM) response has been one of the driving forces in the development of cluster chemistry in the past decade, and the study of ligands potentially able to generate high-nuclearity or high-spin systems is a continuous challenge for synthetic chemists.

Phosphonate ligands are able to link a large number of cations by employing their three potentially bridging O-donor atoms, often allowing high-dimensional networks with interesting application as porous metal−organic frameworks.3 In contrast, NiII molecular systems derived from these kinds of ligands are scarce, and only in the past few years have synthetic strategies capable of restricting the dimensionality of the resulting complexes been successfully developed. The most fruitful strategy consists of the addition of adequate coligands to block some coordination positions of the metallic centers, reducing the polymerization process and providing adequate solubility in common organic solvents. Following this strategy, Winpenny et al. have reported a series of octa-, nona-, deca- and dodecanickel clusters4 and heterometallic {MIII6Ni6} (MIII= Y, Gd, Dy)5 systems employing a RPO3 2−/pivalate blend of ligands.

Recently, other authors have characterized new molecular nickel systems from RPO3 2−/pivalate (Ni8 and Ni10)6 and RPO3 2−/calixarene (Ni8, Ni12, and Ni16) mixtures of ligands.7 Another successful strategy has been the employment of functionalized8 phosphonates or its combination with polyoxometallates. 9

Our previous recent research has been focused on the rich chemistry of first-row transition-metal clusters derived from 2- pyridyloximes, and we have reported a large number of nickel clusters with nuclearities comprised between Ni3 and Ni14.10 In addition to its ability as an efficient superexchange pathway, inducing moderately strong antiferromagnetic coupling, the oximate function tends to generate polynuclear systems employing a variety of coordination modes that can link up to four cations.11 To our knowledge, only two Ni2 and Ni3 mixed oximate/FPO3 2− complexes have recently been reported by one of the authors.12 The oximate ligands in these compounds are neutral, and they contain exclusively fluorophosphate bridges.

On these premises, we decided to combine both kinds of ligands and to explore the 2-pyridyloximate/phosphonate blend with NiII cations, in order to try to generate molecular phosphonate clusters with new topologies and, for the first time, both kinds of bridges. Selected ligands were phenyl-phosphonate (PhPO3 2−) and 6-methyl-2-pyridylaldoxime (6- MepaoH) (Chart 1).

This synthetic strategy successfully yielded several molecular clusters with the formulas [Ni4 (6 -MepaoH)4(PhPO3)2(OH)2(MeOH)4](OH)2·3MeOH (1·3MeOH), [Cs2Ni6(6-

epao)6(PhPO3)3(OH)2(H2O)8]·7H2O (2·7H2O), Cs[Ni8(6-MepaoH)6(6-Mepao)6(PhPO3)3]-(ClO4)5·MeOH (3·MeOH), and [Ni8Na2(BzO)6(6-Mepao) 6(PhPO3)3]·6H2O (4·6H2O). The reported complexes join the scarce number of discrete NiII clusters containing phosphonate ligands and prove their ability to generate new systems with unusual architectures and new cores. Complexes 2−4 contain interesting metallacrown fragments that become determinant in their magnetic response.

.

EXPERIMENTAL SECTION

6-Methylpyridinecarboxaldehyde was purchased from TCI Chemicals, and hydroxylamine hydrochloride and the nickel salts were purchased from Sigma-Aldrich Inc. and used without further purification. The Ni(BzO)2·xH2O starting salt was synthesized by dissolving equimolar amounts (40 mmol) of benzoic acid and sodium hydroxide in 40 mL of water, filtering, and mixing the final solution with a commercial source of Ni(NO3)2·6H2O (20 mmol) in 20 mL of water. After cleaning with water to remove soluble anions, the resulting nickel salt was obtained as a green powder in high yield (>80%). The 6-MepaoH ligand was synthesized as previously reported.10f In all cases, after mixing of the reactants, a large amount of unidentified greenish powder precipitates (probably polymeric products). Consequently, the yields for 1−4 were low, with values of around 15% of well-formed crystals that were employed in the instrumental measurements.

[Ni4(6-MepaoH)4(PhPO3)2(OH)2(MeOH)4](OH)2·3MeOH (1· 3MeOH). 6-Methyl-2-pyridylaldoxime (6-MepaoH; 0.136g, 1 mmol), Ni(BF4)2·6H2O (0.340 g, 1 mmol), Et3N (0.202 g, 2 mmol), and H2PhPO3 (0.4 g, 0.25 mmol) were dissolved in 30 mL of methanol (MeOH). The mixture was stirred for 2 h and then filtered. Crystals were obtained by layering the final solution with 15 mL of diethyl ether. Green crystals adequate for X-ray diffraction formed after 3 weeks. Anal. Calcd for C47H74N8Ni4O21P2 (1·3MeOH): C, 40.79; H, 5.39; N, 8.10. Found: C, 40.3; H, 5.6; N, 8.3. Relevant IR bands (cm−1): 3508 (br), 2584 (br), 1648 (m), 1604 (m), 1519 (m), 1135 (m), 1086 (s), 1048 (s), 1009 (s), 984 (s), 527 (m).

Cs2[Ni6(6-Mepao)6(PhPO3)3(OH)2(H2O)8]·7H2O (2·7H2O). A total of 30 mL of MeOH was poured over 6-MepaoH (0.136 g, 1 mmol), Ni(bzO)2·xH2O (0.301 g, 1 mmol), H2PhPO3 (0.8 g, 0.5 mmol), and CsOH (0.34 g, 2 mmol). The mixture was stirred for 2 h, then filtered, and finally layered with 15 mL of diethyl ether. Brown crystals were collected after 1 month. Anal. Calcd for C60H91N12Cs2Ni6O32P3 (2·7H2O): C, 32.74; H, 4.08; N, 7.64. Found: C, 32.2; H, 3.9; N, 7.3. Relevant IR bands (cm−1): 3396 (br), 1602 (s), 1539 (s), 1462 (m), 1124 (s), 1090 (s), 1048 (s), 974 (s), 706 (m), 665 (m), 561 (m), 550 (m).

Cs[Ni8(6-MepaoH)6(6-Mepao)6(PhPO3)3](ClO4)5·MeOH (3· MeOH). 6-MepaoH (0.136 g, 1 mmol) was dissolved in 30 mL of MeOH with Ni(ClO4)2·6H2O (0.365 g, 1 mmol), H2PhPO3 (0.4 g, 0.25 mmol), and CsOH (0.25 g, 1.5 mmol). The mixture was stirred for 2 h and filtered. Green crystals adequate for X-ray diffraction appeared after 2 weeks of layering of the solution with 15 mL of diethyl ether. Anal. Calcd for C103H109Cl5CsN24Ni8O42P3 (3·MeOH): C, 38.33; H, 3.40; N, 10.41. Found: C, 38.0; H, 3.6; N, 10.7. Relevant IR bands (cm−1): 3417 (br), 3076 (br), 1609 (s), 1557 (s), 1509 (s), 1467 (m), 1335 (m), 1052 (s), 1005 (s), 956 (m), 792 (m), 668 (m), 656 (m), 624 (m), 574 (m), 548 (m).

[Ni8Na2(6-MepyCNO)6(PhPO3)3(BzO)6]·6H2O (4·6H2O). 6-MepaoH (0.136 g, 1 mmol) was dissolved in 30 mL of MeOH with Ni(bzO)2 (0.301 g, 1 mmol), Na(bzO) (0.089 g, 0.5 mmol),

H_2PhPO_3 (0.8 g, 0.5 mmol), and NEt_3 (0.202 g, 2 mmol). The mixture was stirred for 2 h and then filtered. Crystals were obtained by layering the final solution with 15 mL of diethyl ether. Crystals were collected after 1 month. Anal. Calcd for $C_{102}H_{97}N_{12}Na_2Ni_8O_{16.5}P_3$ (4·6H2O): C, 46.63; H, 3.72; N, 6.40. Found: C, 46.2; H, 3.9; N, 6.2. Relevant IR bands (cm^{-1}): 3418 (br), 1600 (m), 1594.32 (w), 1556 (m), 1532 (m), 1107 (s), 1088 (s), 726 (m), 554 (m).

Physical Measurements. Magnetic susceptibility measurements were carried out on polycrystalline samples with a MPMS5 Quantum Design susceptometer working in the range 30−300 K under an external magnetic field of 0.3 T and under a weaker field of 0.03T in the 30−2 K range to avoid saturation effects. Diamagnetic corrections were estimated from Pascal Tables. IR spectra (4000−400 cm^{-1}) were recorded from KBr pellets on a Bruker IFS-125 FT-IR spectrophotometer.

X-ray Crystallography. Details of crystal data, data collection, and refinement for 1−4 are given in Table 1. Collection of the data for compounds 1−4 was made on a Bruker D8 Venture system equipped with a multilayer monochromator and a Mo microfocus (λ = 0.71073 Å). All structures were solved using the Bruker SHELXTL software package and refined with the SHELXL computer program.14 Data were corrected for absorption effects using the multiscan method (SADABS).

All data can be found in the supplementary crystallographic data for this paper in CIF format as CCDC 1434930−1434933 (Supporting Information). These data can be obtained free of charge from The Cambridge Crystallographic Data Centre via www.ccdc.cam.ac.uk/ data_request/cif.

Plots for publication were generated with ORTEP3 for Windows and plotted with Pov-Ray programs.15

RESULTS AND DISCUSSION

Description of the Structures. 1·3MeOH. A view of complex 1 is illustrated in Figure 1. Selected interatomic distances and angles for 1 are listed in Table 2. The core of the tetranuclear cationic compound can be described as two {Ni2(6-MepaoH)2(OH)(MeOH)2}3+ dimers linked by two 4.211 phosphonate ligands. Each NiII cation is coordinated by the two N atoms of one neutral 6-MepaoH, one MeOH molecule, one bridging hydroxo ligand, and three O atoms from two phosphonates, resulting in a NiN2O4 environment. The Ni cations in each dinuclear unit are linked by one μ-OH ligand [Ni(1)−O(1)−Ni(2) 105.3(2)°], one O phosphonate [Ni(1)−O(6′)−Ni(2) 93.4(1)°], and one additional phosphonate bridge. Four strong intramolecular hydrogen bonds between the neutral oximes and O(4) and O(5) contribute to stabilizing the tetranuclear unit.

Charge balance is achieved by means of two hydroxo anions, which give a set of intermolecular hydrogen bonds involving the coordinated MeOH molecules, resulting a one-dimensional (1D) arrangement of tetranuclear clusters.

2·7H2O. The core of compound 2 can be envisaged as two μ3-OH-centered triangular {Ni3(6-Mepao)3(OH)}2+ subunits linked by three phosphonate ligands (Figure 2). Selected interatomic distances and angles for 2 are listed in Table 3.

The two triangular subunits are similar but not identical: coordination of the μ3-OH and oximate ligands gives a inverse [9-MCNiII(6-Mepao)-3] metallacrown with similar bond parameters on both sides of the molecule, but the two remaining coordination sites of each Ni(1,2,3) are fulfilled by O atoms from two different phosphonates, whereas for Ni(4,5,6), they are occupied by one O phosphonate atom and one water molecule, resulting in a common NiN2O4 environment. The water molecules linked to Ni(4,5,6) establish strong hydrogen bonds, with the O atoms of the phosphonate anions stabilizing the cage (Figure 2).

Ni−O−N−Ni torsion angles are between 16.2(5) and 31.3(5)°, being larger in the Ni(4,5,6) unit than in the Ni(1,2,3) unit. Ni−O−Ni bond angles involving the μ3-OH donors are in a short range around 111.5(2)−114.9(2)°. All Ni···Ni distances are very close to 3.4 Å. Each inverse metallacrown links in a direct fashion one Cs+ cation by means of the O oximate atoms, resulting in an octanuclear Cs2Ni6 cluster.

Coordination around the Cs+ cations is completed by four water molecules, which act as bridges with the neighboring Cs+ cations, giving a 1D {Cs2Ni6}n chain of clusters (Figure 3). Coordination around the Cs+ ions consists of four bridging water molecules and three O oximate atoms.

3·MeOH. Compound 3 can be described as two {Ni4(MepaoH)3(Mepao)3}5+ tetrahedral subunits linked by means of three 4.211 phenylphosphonates (PhPO3 2−), as shown in Figure 4. Selected distances and angles for 3 are listed in Table 4. As occurs in compound 2, three deprotonated oximes and three NiII cations form a [9-MCNiII(6-Mepao)-3] metallacrown, which coordinates one NiII cation, giving the two Ni(1,1′,1″,3) and Ni(2,2′,2″,4) tetrahedral subunits. The 6-Mepao− ligands employ a

3.211 coordination mode. The neutral 6-MepaoH ligands are coordinated to Ni(1,2) and symmetry equivalents in its 1.011 mode, acting as a chelate with their N-atom donors. The neutral oxime group establishes a strong hydrogen bond with one of the O phosphonate atoms, helping to stabilize the cluster cage. Both Ni4 moieties are linked by means a triple O phosphonate bridge between the central Ni(3) and Ni(4) ions and three anti−anti phosphonato bridges between the Ni(1) and Ni(2) cations (Figure 4). Thus, each phosphonate ligand coordinates four Ni cations. The charge balance is fulfilled by five perchlorate counteranions and one Cs+ cation.

[Ni8Na2(6-MepyCNO)6(PhPO3)3(BzO)6]·6H2O (4·6H2O). The octanuclear {Ni8(PhPO3)3(Mepao)6}6+ core of the structure of 4 is identical with the above-described complex 3. Selected distances and angles for 4 are listed in Table 5, and a view of the complex is given in Figure 5. The differences between the two compounds lie in substitution of the neutral MepaoH ligands in 3 by six benzoates in 4, resulting in a NiN3O3 environment for Ni(2) and symmetry-related cations. The O(2) benzoate atoms and O(1) oximate donors link one Na+ cation, resulting in a decanuclear {Na2Ni8} cluster. Ni−O− N−Ni torsion angles and Ni···Ni distances are also very similar to the above compound. In this case, the six benzoates and two Na+ cations fulfill the charge balance, resulting in a neutral cluster.

Comments on the {Ni3(Mepao)3}3+ Metallacrowns. Oximate ligands are some of the classical ligands capable of generating metallacrowns, with the {−M−N−O−}n fragment as the repeating unit.16 The O atoms of the oximate ligands can coordinate additional cations, and for n = 4 or 5, a large number of compounds have been reported with one cation in the center of the ring (Chart 2). According to the size of the metallacycle, transition cations are preferred when n = 4 and lanthanides when n = 5.15

In contrast, for n = 3, the most common situation (more than 300 CCDC entries) is the inverse metallacrown, in which the center of the triangle is occupied by one anionic group, typically oxo, hydroxo, alkoxo, or halides in some cases (Chart 2), with the coordination of cations being extremely unusual. The only available examples of the coordination of additional cations are given for one homometallic tetranuclear system in which one FeIII cation is coordinated by one [9-MCFeIII(NO)-3] metallacrown, 17 one heterometallic tetramer showing one CrIII cation linked by one [9-MCMnIII(NO)-3] metallacrown,18 or one sandwich-like heptanuclear system with one MnII linked by two (μ3-O)[9-MCMnIII(NO)-3] inverse metallacrowns.19

Compounds 2−4 exhibit {−M−N−O−}3 metallacycles in three different situations (Figure 6). In complex 2, the inverse (μ3-OH)[9-MCNiII-3] links one Cs+ cation in a direct fashion. The OH− ligands are placed 0.492 and 0.570 Å out of the main Ni(1,2,3) or Ni(4,5,6) planes, respectively, whereas in the opposite sense, the O oximate donors link the Cs+ ion. The oximato ligands are strongly displaced from the metal planes, as shown by the distances between the mean O oximato and Ni planes, which reach 1.545 and 1.460 Å. The Cs+ ions are placed 2.281 and 2.225 Å, respectively, from the centroid of the Oatom donors.

In complex 3, the metallacrowns link one NiII cation, placed 1.77 Å from the centroid of the ring. The distance between Ni and O oximato mean planes is 0.582 Å. Each [9-MCNiII-3] ring in complex 4 links one NiII cation with bond parameters very similar to those in 3, but in this case, the metallacrowns also link one Na+ cation in the opposite face of the cycle, resulting in a unique case of the simultaneous linkage of two cations at both sides of the {Ni−O−N−}3 metallamacrocyclic unit.

As could be expected, the {Ni−O−N−}3 rings in complexes 3 and 4 are flattened in comparison with the inverse metallacrown in 2 (Figure 6).

Magnetic Measurements and Modeling. The numbering of all of the spin carriers in the applied Hamiltonians and in the subsequent discussion for 1−4 is provided in Chart 3. The fit of the experimental data was made for all complexes using the PHI program20 and applying the Hamiltonians derived from the corresponding interaction scheme. The quality of the fits is parametrized as the factor R = (χMTexp − χMTcalc)2/ (χMTexp)2.

The room temperature χMT value for 1 is 4.79 cm3 K mol−1, slightly larger than the expected value for four isolated S = 1 local spins. This value remains practically constant in the 300− 75 K range, and below this temperature, it decreases continuously to 0.42 cm3 K mol−1 at 2 K (Figure 7). The susceptibility plot exhibits a maximum at 8 K, indicating dominant antiferromagnetic interactions and an S = 0 ground state.

The system shows six interaction pathways that can be modeled with two coupling constants tending to the kinds of bridges and the symmetry of the cluster: one constant for the double-oxo/phosphonate bridges (J1) and a second one for the four single phosphonate bridges (J2). The corresponding Hamiltonian was

$$H = -J_1(S_1 \cdot S_2 + S_3 \cdot S_4) - J_2(S_1 \cdot S_3 + S_1 \cdot S_4 + S_2 \cdot S_3 + S_2 \cdot S_4)$$

The best-fit parameters were J1 = +3.1 cm−1, J2 = −3.0 cm−1, and g = 2.22, with R = 1.70 × 10−5. Calculation of the energy of the lower spin states indicates an S = 0 ground state, followed by one S = 1 and one S = 2 with gaps of 2.96 and 8.87 cm−1, respectively. Magnetization experiments show a nonsaturated value equivalent to 2.55 electrons, consistent with the partial population of the S = 1 and 2 low-lying ground states under high fields. Magnetic measurements on previously reported systems containing solely Ni−O−P−O−Ni bridges show weak antiferromagnetic coupling in good agreement with the sign and magnitude of J2.12

Compound 2 shows a room temperature χMT value of 6.37 cm3 K mol−1, which decreases continuously upon cooling and tends to zero at low temperature (Figure 7). The core of 2 is very irregular, with six similar but not identical Ni−N−O−Ni torsion angles and two phosphonate pathways. To avoid overparametrization, a very simplified scheme with only two coupling constants was assumed, J1

corresponding to the six Ni−N−O−Ni interactions and J2 = J3 common to all phosphonate bridges. According to Chart 3, the fit was performed by applying the Hamiltonian

$$H = -J_1(S_1 \cdot S_2 + S_1 \cdot S_3 + S_2 \cdot S_3 + S_4 \cdot S_5 + S_4 \cdot S_6 + S_5 \cdot S_6) - J_2(S_1 \cdot S_4 + S_2 \cdot S_6 + S_3 \cdot S_5 + S_1 \cdot S_5 + S_2 \cdot S_4 + S_3 \cdot S_6)$$

The best-fit parameters were J1 = −25.8 cm−1, J2 = −0.9 cm−1, and g = 2.22, which in spite of the reduced model give a good fit of the experimental data with R = 9.0 × 10−4. Density functional theory calculations on triangular nickel oximato complexes with a central μ-OH ligand previously reported by us show little dependence on the antiferromagnetic interaction with the Ni−O−N−Ni torsion angle and a strong dependence on the Ni−O−Ni bond angle, with the maximum for planar systems being the 120° angle.10g The obtained J1 = −25.8 cm−1 value agrees with the expected range of values for moderate bond angles of 111.5−114.9°.

Complexes 3 and 4 show a common core from a magnetic point of view, and their description and fits can be performed by applying the same interaction scheme (Chart 3, bottom). The χMT products at room temperature for compounds 3 and 4 are 7.93 and 7.55 cm3 K mol−1, respectively. These values are slightly lower than those expected for eight noninteracting S = 1 local spins. Upon cooling, both plots decay monotonically and tend to zero at low temperatures. The presence of a rounded susceptibility maximum at 35 K for 3 and 45 K for 4 confirms an S = 0 ground state and overall moderately strong antiferromagnetic interactions (Figure 7).

Analysis of the structures of 3 and 4 reveals 22 superexchange pathways that can be described as 5 different interactions: the central spin carriers S4 and S5 are bridged by three oxo bridges from phosphonate donors (J1), each triangular subunit is linked by means of oximato bridges to the central S4 or S5 with large Ni−O−N−Ni torsion angles (J2), the two triangular S1/S2/S3 and S4/S5/S6 subunits are linked by identical oximate bridges (J3), and finally the phosphonate anions link both triangular subunits between them (J4) and S1/ S2/S3 and S4/S5/S6 subunits with S5 and S4, respectively (J5), summarizing up to 22 superexchange pathways. From this scheme, a five-J Hamiltonian can be built:

$$H = -J_1(S_4 \cdot S_5) - J_2(S_1 \cdot S_4 + S_2 \cdot S_4 + S_3 \cdot S_4 + S_5 \cdot S_6 + S_5 \cdot S_7 + S_5 \cdot S_8) - J_3(S_1 \cdot S_2 + S_1 \cdot S_3 + S_2 \cdot S_3 + S_6 \cdot S_7 + S_6 \cdot S_8 + S_7 \cdot S_8) - J_4(S_1 \cdot S_6 + S_2 \cdot S_7 + S_3 \cdot S_8) + J_5(S_1 \cdot S_5 + S_2 \cdot S_5 + S_3 \cdot S_5 + S_4 \cdot S_6 + S_4 \cdot S_7 + S_4 \cdot S_8)$$

Very good fits could be obtained for a number of sets of J1−J5 values when the complete Hamiltonian was applied, evidencing overparametrization. However, all performed fits showed some constant trends:

as expected, interactions mediated by oximato bridges were always antiferromagnetic and much larger than the interactions mediated by the phosphonate bridges in all fits ($|J2, J3| \gg |J1, J4, J5|$). This fact confirms that J1, J4, and J5 are only operative at low temperatures.

To reduce the overparametrization and taking into account the low values of J obtained for the Ni−OPO−Ni pathways in compounds 1 and 2, the fit of the experimental data was performed by discarding the J4 and J5 interactions. Excellent fits for the complete range of temperatures were obtained for the parameters J1 = −11.0 cm−1, J2 = −33.6 cm−1, J3 = −51.0 cm−1, and g = 2.45 for 3 and J1 = −12.2 cm−1, J2 = −35.0 cm−1, J3 = −51.2 cm−1, and g = 2.39 for 4 with $R = 1.5 \times 10^{-5}$ and 8.2×10^{-5}, respectively.

Previously reported phosphonato clusters with higher nuclearities have a large number of potential superexchange pathways, and often a fit of the experimental data has not been reported because overparametrized Hamiltonians tend to give good fits for different sets of coupling constants, resulting in poorly reliable J values. However, in our case, the reported clusters contain two very different kinds of bridges: oximato ligands give equilateral triangular NiII 3 subunits for 2 and tetrahedral Ni4 subunits for 3 and 4 further linked by a complex set of phosphonate linkages. The interaction mediated by the oximate pathways, with moderate Ni−N−O−Ni torsion angles,10e is always strongly antiferromagnetic, and the ground state for the equilateral triangular or tetrahedral NiII topologies must be a local S = 0. In contrast, the interactions mediated by the phosphonate bridges are always weak (ferromagnetic or antiferromagnetic), being only relevant at low temperature, and thus it becomes difficult to calculate when the system is close to diamagnetism.

Obviously, for such complicated systems, the absolute values of the coupling constants are only an approach to the real values. However, all data for complexes 2−4 converge in the same general conclusion: the main factor that determines the antiferromagnetic interactions is the interaction mediated for the oximato bridges, which by itself (as occurs for equilateral triangles or tetrahedra) determines a S = 0 ground state for the three complexes.

CONCLUSIONS

Employment for the first time of a 6-MepaoH/PhPO32− blend of ligands with Ni2+ salts has led to four new Ni4, Cs2Ni6, Ni8, and Na2Ni8 clusters with unprecedented cores. Complexes 2−4 have provided rare examples of clusters built on linked metallacrowns and their coordination to Cs+, Na+, or NiII cations.

Magnetic measurements carried out in the 300−2 K range revealed antiferromagnetic response for 1−4, clearly dominated by the efficient oximato superexchange pathway. A blend of phosphonato ligands with other coligands is a promising way to generate new cluster topologies with large nuclearities.

AUTHOR INFORMATION

Corresponding Author

*E-mail**:** albert.escuer@ub.edu.

Author Contributions

The manuscript was written through contributions of all authors.

Notes

The authors declare no competing financial interest.

ACKNOWLEDGEMENTS

Funds from the CICYT Project CTQ2015-63614-P are acknowledged.

REFERENCES

(1) (a) Rosa, D. T.; Krause Bauer, J. A.; Baldwin, M. J. Inorg. Chem. 2001, 40, 1606−1613. (b) Akine, S.; Taniguchi, T.; Saiki, T.; Nabeshima, T. J. Am. Chem. Soc. 2005, 127, 540−541. (c) Goldcamp, M. J.; Robison, S. E.; Krause Bauer, J. A.; Baldwin, M. J. Inorg. Chem. 2002, 41, 2307−2309.

(2) (a) Boyd, P. D. W.; Li, Q.-Y.; Vincent, J. B.; Folting, K.; Chang, H. R.; Streib, W. E.; Huffman, J. C.; Christou, G.; Hendrickson, D. N. J. Am. Chem. Soc. 1988, 110, 8537−8539. (b) Milios, C. J.; Inglis, R.; Vinslava, A.; Bagai, R.; Wernsdorfer, W.; Parsons, S.; Perlepes, S. P.; Christou, G.; Brechin, E. K. J. Am. Chem. Soc. 2007, 129, 12505−12511. (c) Choi, H. J.; Sokol, J. J.; Long, J. R. Inorg. Chem. 2004, 43, 1606−1608. (d) Bogani, L.; Wernsdorfer, W. Nat. Mater. 2008, 7, 179−186. (e) Aromı, G.; Parsons, S.; Wernsdorfer, W.; Brechin, E. K.; McInnes, E. J. L. Chem. Commun. 2005, 5038−5040.

(3) (a) Clearfield, A.; Demandis, K. Metal Phosphonate Chemistry: From Synthesis to Applications; The Royal Society of Chemistry: Cambridge, U.K., 2012. (b) Gagnon, K. J.; Perry, H. P.; Clearfield, A. Chem. Rev. 2012, 112, 1034−1054. (c) Shimizu, G. K. H.; Vaidhyanathan, R.; Taylor, J. M. Chem. Soc. Rev. 2009, 38, 1430−1449.

(4) (a) Breeze, B. A.; Shanmugam, M.; Tuna, F.; Winpenny, R. E. P. Chem. Commun. 2007, 5185−5187. (b) Langley, S. K.; Helliwell, M.; Teat, S. J.; Winpenny, R. E. P. Inorg. Chem. 2014, 53, 1128−1134.

(5) (a) Zheng, Y.-Z.; Evangelisti, M.; Winpenny, R. E. P. Angew. Chem., Int. Ed. 2011, 50, 3692−3695. (b) Pineda, E. M.; Tuna, F.; Zheng, Y.-Z.; Winpenny, R. E. P.; McInnes, E. J. L. Inorg. Chem. 2013, 52, 13702−13707.

(6) (a) Burkovskaya, N. P.; Nikiforova, M. E.; Kiskin, M. A.; Pekhn'o, V. I.; Sidorov, A. A.; Novotortsev, V. M.; Eremenko, I. L. Russ. J. Coord. Chem. 2012, 38, 331−336. (b) Sheikh, J. A.; Adhikary, A.; Jena, H. S.; Biswas, S.; Konar, S. Inorg. Chem. 2014, 53, 1606−1613.

(7) Su, K.; Jiang, F.; Qian, J.; Gai, Y.; Wu, M.; Bawaked, S. M.; Mokhtar, M.; Al-Thabaiti, S. A.; Hong, M. Cryst. Growth Des. 2014, 14, 3116−3123.

(8) (a) Cao, D.-K.; Xiao, J.; Li, Y.-Z.; Zheng, L.-M. Chin. J. Inorg. Chem. 2007, 23, 1947−1953. (b) Ma, K.; Xu, J.; Zhang, L.; Shi, J.; Zhang, D.; Zhu, Y.; Fan, Y.; Song, T. New J. Chem. 2009, 33, 886−892. (c) Adelani, P. O.; Oliver, A. G.; Albrecht-Schmitt, T. E. Inorg. Chem. 2012, 51, 4885−4887. (d) Gudima, A.O.; Shovkova, G. V.; Trunova, O. K.; Grandjean, F.; Long, G. J.; Gerasimchuk, N. Inorg. Chem. 2013, 52, 7467−7477.

(9) (a) El Moll, H.; Rousseau, G.; Dolbecq, A.; Oms, O.; Marrot, J.; Haouas, M.; Taulelle, F.; Riviere, E.; Wernsdorfer, W.; Lachkar, D.; Lacote, E.; Keita, B.; Mialane, P. Chem. - Eur. J. 2013, 19, 6753−6765. (b) You, Z.; Chen, Y.; Liu, T.; Yang, Z.; Xie, F.; Sun, Y. Inorg. Chim. Acta 2014, 421, 160−168.

(10) (a) Stamatatos, T. C.; Diamantopoulou, E.; Raptopoulou, C. P.; Psycharis, V.; Escuer, A.; Perlepes, S. P. Inorg. Chem. 2007, 46, 2350−2352. (b) Stamatatos, T. C.; Escuer, A.; Abboud, K. A.; Raptopoulou, C. P.; Perlepes, S. P.; Christou, G. Inorg. Chem. 2008, 47, 11825−11838. (c) Escuer, A.; Esteban, J.; Aliaga-Alcalde, N.; Font-Bardia, M.; Calvet, T.; Roubeau, O.; Teat, S. J. Inorg. Chem. 2010, 49, 2259−2266. (d) Papatriantafyllopoulou, C.; Stamatatos, T.; Wernsdorfer, W.; Teat, S. J.; Tasiopoulos, A.; Escuer, A.; Perlepes, S. P. Inorg. Chem. 2010, 49, 10486−10496. (e) Escuer, A.; Esteban, J.; Roubeau, O. Inorg. Chem. 2011, 50, 8893−8901. (f) Escuer, A.; Vlahopoulou, G.; Mautner, F. A. Dalton Trans. 2011, 40, 10109−10116. (g) Esteban, J.; Ruiz, E.; Font-Bardia, M.; Calvet, T.; Escuer, A. Chem. - Eur. J. 2012, 18, 3637−3648. (h) Esteban, J.; Alcázar, L; Torres-Molina, M.; Monfort, M.; Font-Bardia, M.; Escuer, A. Inorg. Chem. 2012, 51, 5503−5505. (i) Escuer, A.; Esteban, J.; Font-Bardia, M. Chem. Commun. 2012, 48, 9777−9779. (j) Esteban, J.; Font-Bardia, M.; Escuer, A. Eur. J. Inorg. Chem. 2013, 2013, 5274−5280. (k) Esteban, J.; Font-Bardia, M.; Escuer, A. Inorg. Chem. 2014, 53, 1113−1121. (l) Esteban, J.; Font-Bardia, M.; Costa, J. S.; Teat, S. J.; Escuer, A. Inorg. Chem. 2014, 53, 3194−3203. (m) Escuer, A.; Esteban, J.; Mayans, J.; Font-Bardia, M. Eur. J. Inorg. Chem. 2014, 2014, 5443−5450.

(11) Milios, C. J.; Stamatatos, T. C.; Perlepes, S. P. Polyhedron 2006, 25, 134−194.

(12) Dermitzaki, D.; Raptopoulou, C. P.; Psycharis, V.; Escuer, A.; Perlepes, S. P.; Stamatatos, T. C. Dalton Trans. 2014, 43, 14520−14524.

(13) Coxall, R. A.; Harris, S. G.; Henderson, D. K.; Parsons, S.; Tasker, P. A.; Winpenny, R. E. P. J. Chem. Soc., Dalton Trans. 2000, 2349−2356.

(14) Sheldrick, G. M. Acta Crystallogr., Sect. A: Found. Crystallogr. 2008, 64, 112−122.

(15) ORTEP-3 for Windows: Farrugia, L. J. J. Appl. Crystallogr. 1997, 30, 565.

(16) Mezei, G.; Zaleski, C. M.; Pecoraro, V. L. Chem. Rev. 2007, 107, 4933−5003.

(17) Lah, M. S.; Kirk, M. L.; Hatfield, W.; Pecoraro, V. L. J. Chem. Soc., Chem. Commun. 1989, 1606−1608.

(18) Khanra, S.; Biswas, B.; Golze, C.; Buchner, B.; Kataev, V.; Weyhermuller, T.; Chaudhuri, P. Dalton Trans. 2007, 481−487.

(19) Milios, C. J.; Gass, I. A.; Vinslava, A.; Budd, L.; Parsons, S.; Wernsdorfer, W.; Perlepes, S. P.; Christou, G.; Brechin, E. K. Inorg. Chem. 2007, 46, 6215−6217.

(20) Chilton, N. F.; Anderson, R. P.; Turner, L. D.; Soncini, A.; Murray, K. S. J. Comput. Chem. 2013, 34, 1164−1175.

.

Legends to figures

Chart 1. PhPO3 2− and 6-MepaoH Ligands and Their Coordination Modes Found in Compounds 1−4 (in Harris Notation13)

Figure 1. (Left) Partially labeled molecular structure of complex 1. (Right) View of the intermolecular hydrogen bonds that determine the arrangement of molecules in the crystal. Color key: NiII, green; O, red, N, navy blue; P, orange.

Figure 2. (Top) View of complex 2. (Bottom) Partially labeled plot of the Ni6 core of complex 2. Intramolecular hydrogen bonds are plotted as red dashed lines.

Figure 3. 1D arrangement of Ni6 clusters linked by Cs+ cations in compound 2.

Figure 4. (Top) View of compound 3. (Bottom) Partially labeled plot of the core of complex 3.

Figure 5. (Top) View of the molecular unit of compound 4. (Bottom) Partially labeled plot of the decanuclear core of complex 4, showing coordination of the Na+ cations.

Chart 2. Schematic Plot of the Most Common Inner Coordination for Oximate Metallacycles

Figure 6. (Top) View of the {Ni3(Mepao)3}3+ metallacrown present in compounds 2−4. (Bottom) OH− and Cs+ (2), NiII (3), or NiII and NaI (4) ions linked to the metallacrowns.

Chart 3. Schematic of All of the Magnetic Interactions for Compounds 1 (Top, Left), 2 (Top, Right), and 3 and 4 (Bottom) (See the Text for the Corresponding Hamiltonians)

Figure 7. Product of χM versus T (left) and χMT versus T (right) for compounds 1 (triangles, black), 2 (diamonds, green), 3 (dot-centered squares, blue), and 4 (dot-centered circles, red). Solid lines show the best fits.

CHART 1.

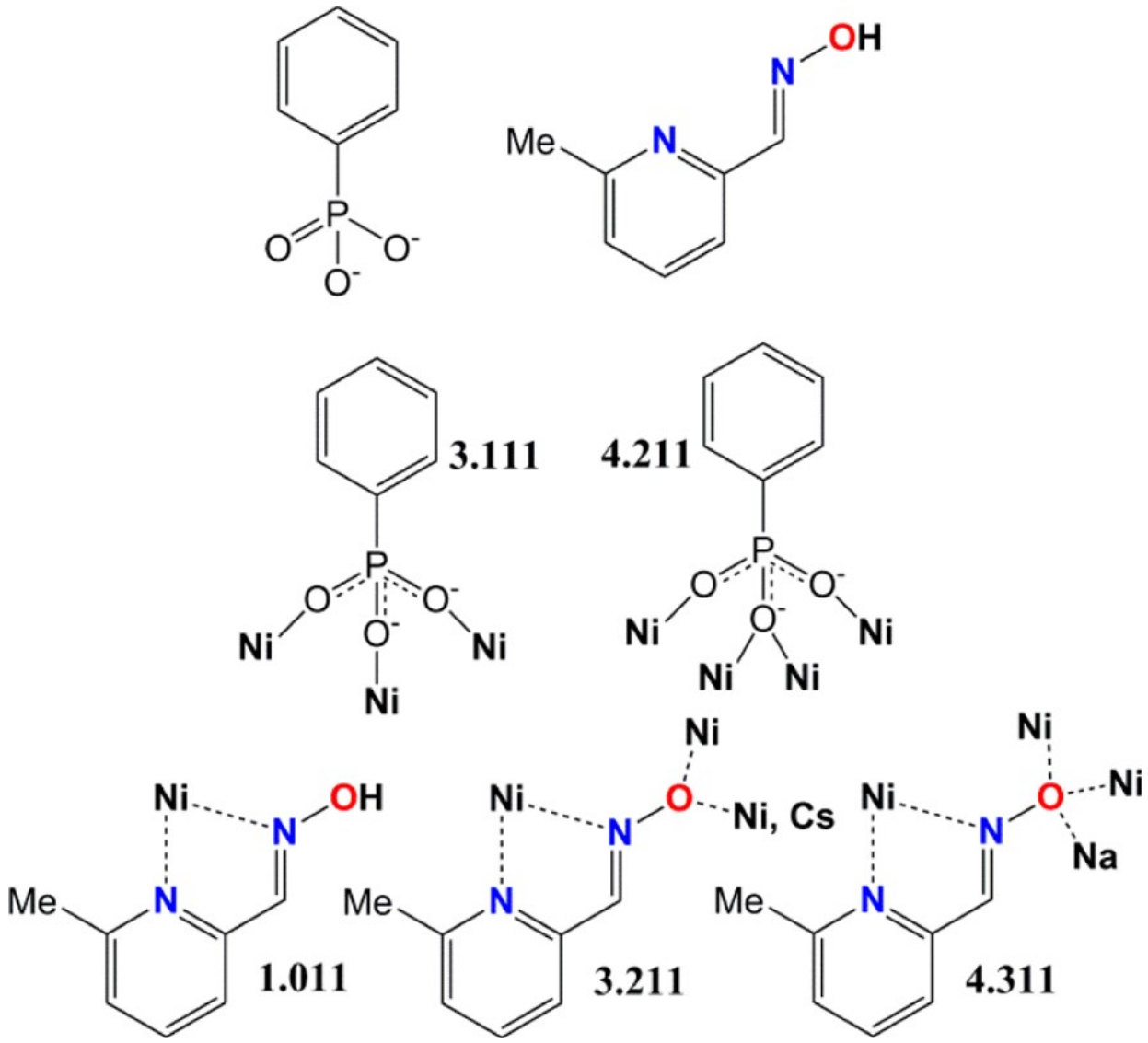

FIGURE 1.

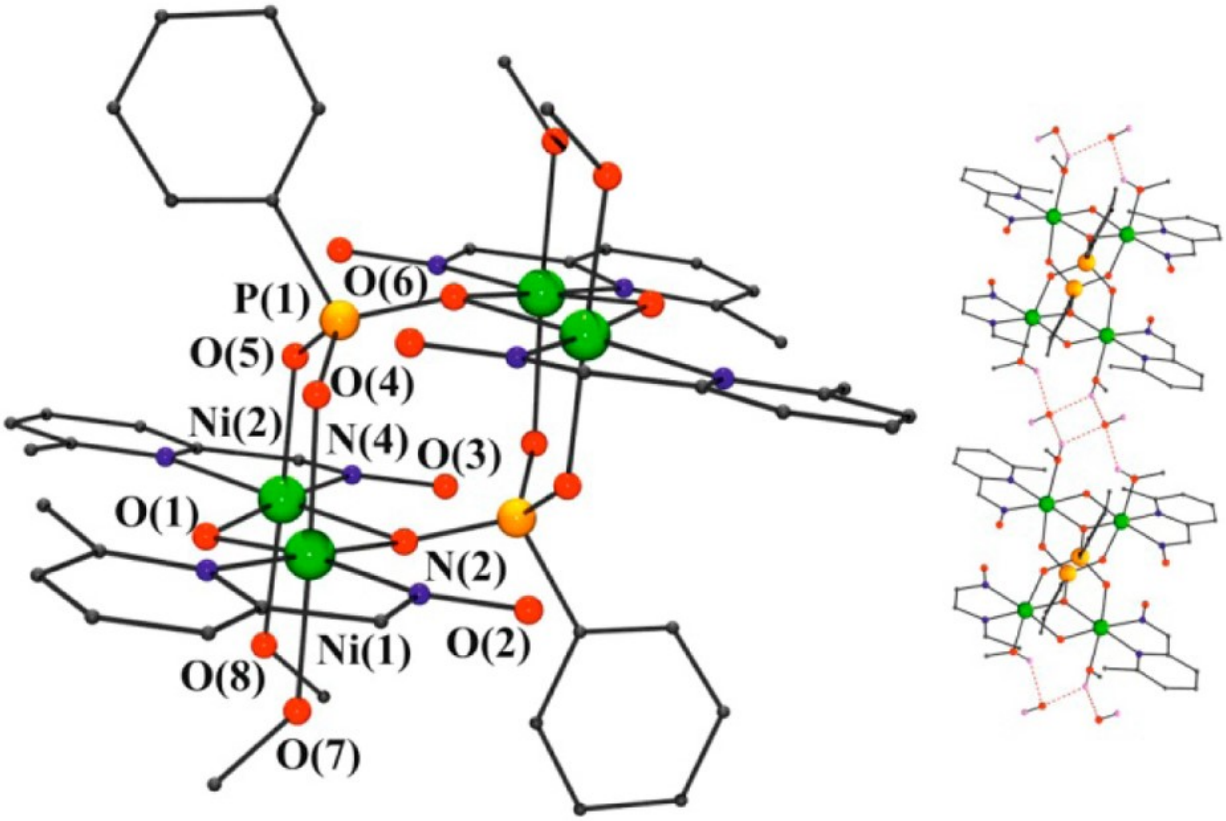

FIGURE 2.

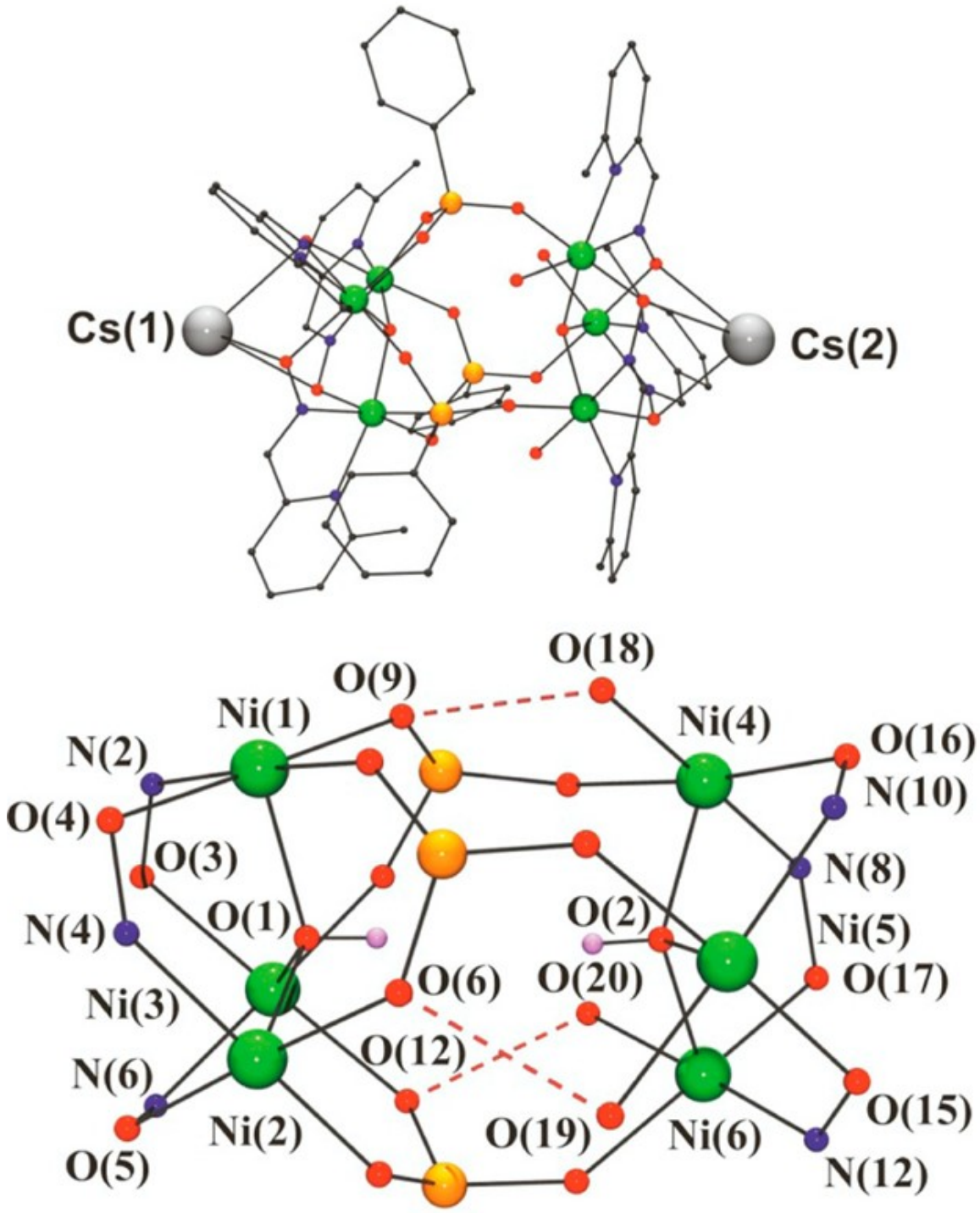
Cs(1)
Cs(2)
O(18)
O(9)
Ni(1)
Ni(4)
O(16)
N(2)
N(10)
O(4)
O(3)
N(8)
N(4)
O(1)
O(2)
Ni(5)
O(6)
O(20)
O(17)
Ni(3)
O(12)
N(6)
O(15)
Ni(2)
O(19)
Ni(6)
O(5)
N(12)

FIGURE 3.

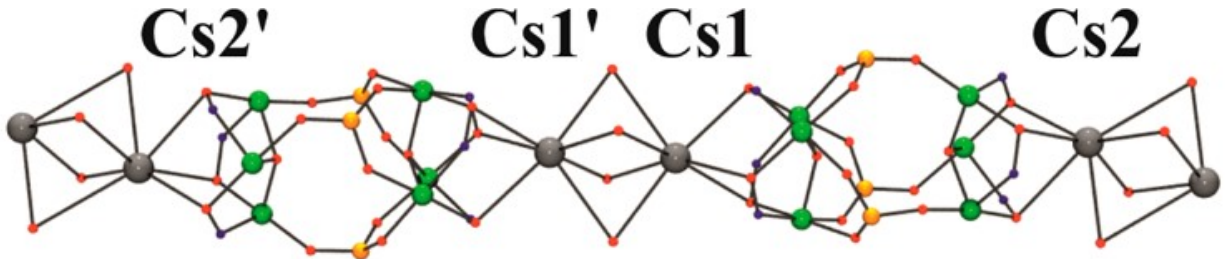

FIGURE 4.

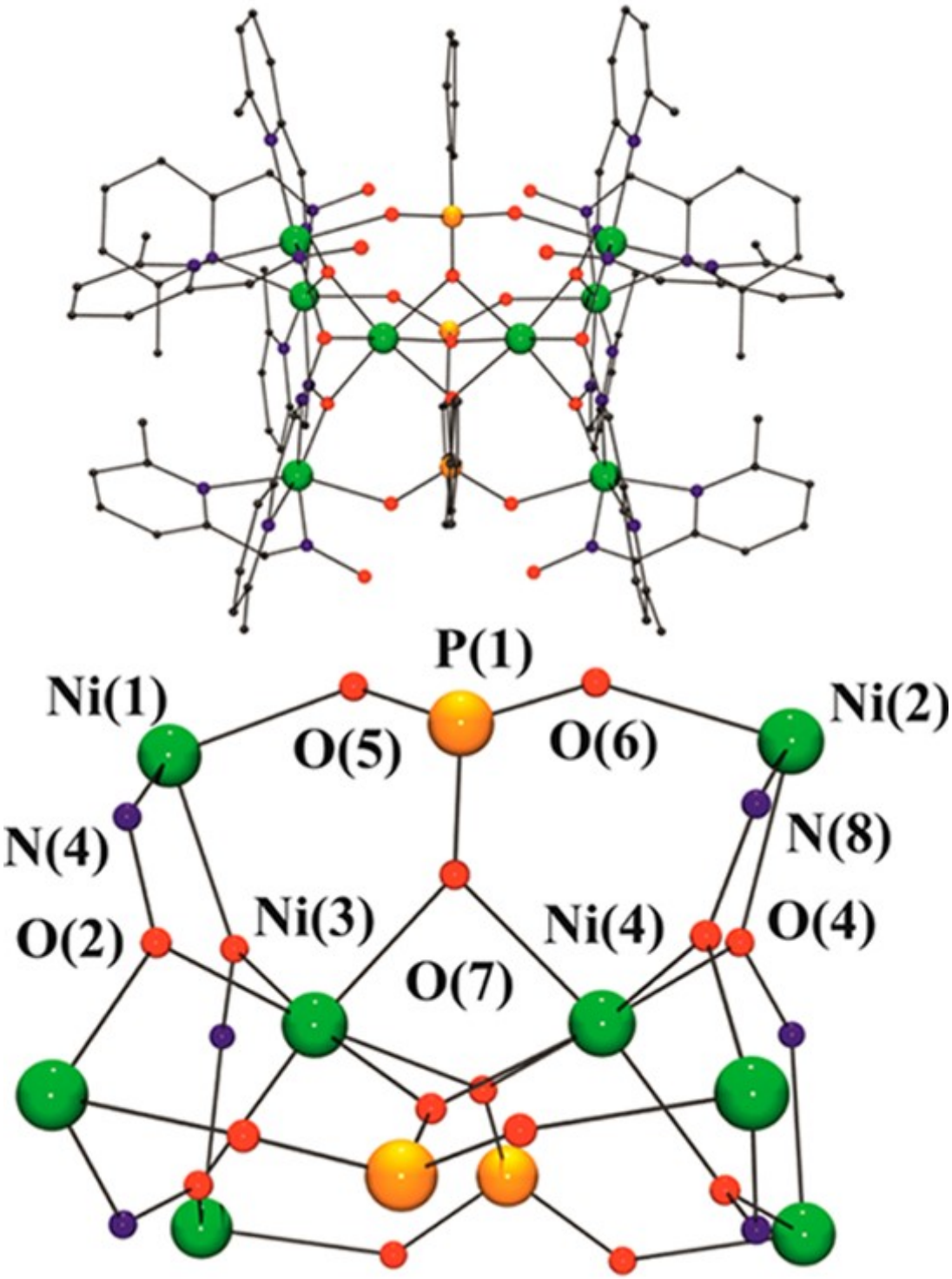

Table 1. Crystal Data, Data Collection, and Structure Refinement Details for the X-ray Structure Determination of Compounds **1**−**4**

	1 (Ni_6)	**2** (Ni_6Cs_2)	**3** (Ni_8Cs)	**4** (Ni_8Na_2)
formula	$C_{47}H_{68}N_8Ni_6O_{21}P_2$	$C_{49}H_{91}Cs_2N_{12}Ni_6O_{32}P_3$	$C_{103}H_{109}Cl_5CsN_{24}Ni_8O_{42}P_3$	$C_{204}H_{195}N_{24}Na_4Ni_{16}O_{66}P_6$
fw	1377.87	2203.43	3227.89	5255.97
system	triclinic	triclinic	cubic	hexagonal
space group	$P\bar{1}$	$P\bar{1}$	$P\bar{2}13$	$P\bar{6}2c$
a, Å	11.802(2)	15.797(2)	23.042(1)	18.6908(8)
b, Å	12.179(2)	16.522(2)	23.042(1)	18.6908(8)
c, Å	12.676(2)	16.532(2)	23.042(1)	22.3049(9)
α, deg	77.751(5)	82.452(5)	90	90
β, deg	77.748(5)	80.595(5)	90	90
γ, deg	63.279(4)	78.461(5)	90	120
V, Å^3	1576.1(3)	4148.9(9)	12234(2)	6748.2(6)
Z	1	2	4	1
T, K	100(2)	100(2)	100(2)	100(2)
λ(Mo Kα), Å	0.71073	0.71073	0.71073	0.71073
ρ_{calc}, g·cm^{-3}	1.452	1.764	1.753	1.293
μ(Mo Kα), mm^{-1}	1.302	2.344	1.741	1.202
R1	0.0597	0.0619	0.0723	0.0391
wR2	0.1614	0.1523	0.2068	0.1100

Table 2. Selected Interatomic Distances (Å) and Angles (deg) for Compound 1

Ni(1)–O(1)	1.963(4)	Ni(2)–O(1)	1.956(4)
Ni(1)–O(4)	2.056(4)	Ni(2)–O(5)	2.066(4)
Ni(1)–O(6')	2.136(4)	Ni(2)–O(6')	2.146(3)
Ni(1)–O(7)	2.086(4)	Ni(2)–O(8)	2.079(4)
Ni(1)–N(1)	2.147(5)	Ni(2)–N(3)	2.160(4)
Ni(1)–N(2)	2.078(4)	Ni(2)–N(4)	2.063(5)
O(3)–N(4)	1.375(6)	P(1)–C(15)	1.825(8)
O(2)–N(2)	1.377(6)	P(1)–O(4)	1.529(4)
Ni(1)–O(1)–Ni(2)	105.3(2)	P(1)–O(5)	1.530(4)
Ni(1)–O(6')–Ni(2)	93.4(1)	P(1)–O(6)	1.532(4)
Intramolecular Hydrogen Bonds			
D–H···A	H···A	D···A	D–H–A
O(2)–H(2)···O(5)	1.81	2.534(5)	146.0
O(3)–H(3)···O(4)	1.82	2.536(6)	145.0

Table 3. Selected Interatomic Distances (Å) and Angles (deg) for Compound 2

Ni(1)–O(1)	2.015(3)	Ni(1)–O(1)–Ni(2)	114.9(2)
Ni(2)–O(1)	2.017(3)	Ni(1)–O(1)–Ni(3)	114.2(2)
Ni(3)–O(1)	2.016(3)	Ni(2)–O(1)–Ni(3)	113.7(2)
Ni(4)–O(2)	2.067(4)	Ni(4)–O(2)–Ni(5)	111.5(2)
Ni(5)–O(2)	2.083(4)	Ni(4)–O(2)–Ni(6)	114.3(2)
Ni(6)–O(2)	2.071(3)	Ni(5)–O(2)–Ni(6)	112.5(2)
Cs(1)–O(3)	3.124(4)	Ni(1)–O(4)–N(4)–Ni(2)	16.7(4)
Cs(1)–O(4)	3.111(4)	Ni(1)–N(2)–O(3)–Ni(3)	18.6(4)
Cs(1)–O(5)	3.127(4)	Ni(2)–O(5)–N(6)–Ni(3)	16.2(5)
Cs(2)–O(15)	3.119(4)	Ni(4)–O(16)–N(10)–Ni(5)	29.5(5)
Cs(2)–O(16)	3.237(4)	Ni(5)–O(15)–N(12)–Ni(6)	31.3(5)
Cs(2)–O(17)	2.920(4)	Ni(4)–N(8)–O(17)–Ni(6)	18.3(5)
O(3)–N(2)	1.339(5)	O(15)–N(12)	1.347(5)
O(4)–N(4)	1.340(5)	O(16)–N(10)	1.337(6)
O(5)–N(6)	1.341(5)	O(17)–N(8)	1.352(5)
Intramolecular Hydrogen Bonds			
D–H···A	H···A	D···A	D–H–A
O(18)–H(*x*)···O(8)	1.83(4)	2.720(5)	171(4)
O(18)–H(*x*)···O(9)	1.80(4)	2.669(5)	159(5)
O(19)–H(*x*)···O(6)	1.78(4)	2.652(5)	165(6)
O(19)–H(*x*)···O(14)	1.95(5)	2.808(5)	159(4)
O(20)–H(*x*)···O(11)	1.99(4)	2.8538(5)	160(4)
O(20)–H(*x*)···O(12)	1.74(4)	2.614(5)	165(6)

Table 4. Selected Interatomic Distances (Å) and Angles (deg) for Compound 3

Ni(1)–O(2′)	2.122(10)	Ni(2)–O(4′)	2.133(9)
Ni(1)–O(5)	2.070(10)	Ni(2)–O(6)	2.053(9)
Ni(1)–N(1)	2.187(13)	Ni(2)–N(5)	2.178(13)
Ni(1)–N(2)	2.054(14)	Ni(2)–N(6)	2.061(13)
Ni(1)–N(3)	2.157(12)	Ni(2)–N(7′)	2.145(11)
Ni(1)–N(4)	2.083(12)	Ni(2)–N(8′)	2.090(11)
Ni(3)–O(2)	2.021(9)	Ni(4)–O(4)	2.020(9)
Ni(3)–O(7)	2.082(9)	Ni(4)–O(7)	2.081(9)
O(2)–N(4)	1.38(2)	O(4)–N(8)	1.37(1)
Ni(1)–O(2′)–Ni(3)	111.9(4)	Ni(1)–N(4)–O(2)–Ni(1′)	141.4(8)
Ni(2)–O(4′)–Ni(4)	112.1(2)	Ni(1)–N(4)–O(2)–Ni(3)	26(1)
Ni(3)–O(7)–Ni(4)	88.1(3)	Ni(2)–N(8)–O(4)–Ni(2′)	140.3(8)
		Ni(2)–N(8)–O(4)–Ni(4)	23(1)

Table 5. Selected Interatomic Distances (Å) and Angles (deg) for Compound 4

Ni(1)–O(1)	2.009(3)	Ni(2)–O(1′)	2.084(3)
Ni(1)–O(4)	2.065(3)	Ni(2)–O(2)	2.191(4)
Na(1)–O(1)	2.572(4)	Ni(2)–O(3)	2.092(4)
Na(1)–O(2)	2.348(4)	Ni(2)–O(5)	1.988(3)
O(1)–N(2)	1.352(5)	Ni(2)–N(1)	2.115(4)
		Ni(2)–N(2)	2.050(4)
Ni(1)–O(4)–Ni(1′)	81.7(2)	Ni(2)–N(2)–O(1)–Ni(1)	32.0(4)
Ni(1)–O(1)–Ni(2′)	110.0(1)	Ni(2)–N(2)–O(1)–Ni(2′)	141.3(3)
Ni(2)–O(2)–Na(1)	91.1(2)		